3018–3028 *Nucleic Acids Research, 1999, Vol. 27, No. 15*

The effect of sodium, potassium and ammonium ions on the conformation of the dimeric quadruplex formed by the *Oxytricha nova* telomere repeat oligonucleotide $d(G_4T_4G_4)$

Peter Schultze, Nicholas V. Hud, Flint W. Smith and Juli Feigon*

Department of Chemistry and Biochemistry and Molecular Biology Institute, University of California, Los Angeles, CA 90095, USA

Received May 11, 1999; Accepted May 28, 1999

ABSTRACT

The DNA sequence $d(G_4T_4G_4)$ [Oxy-1.5] consists of 1.5 units of the repeat in telomeres of *Oxytricha nova* and has been shown by NMR and X-ray crystallographic analysis to form a dimeric quadruplex structure with four guanine-quartets. However, the structure reported in the X-ray study has a fundamentally different conformation and folding topology compared to the solution structure. In order to elucidate the possible role of different counterions in this discrepancy and to investigate the conformational effects and dynamics of ion binding to G-quadruplex DNA, we compare results from further experiments using a variety of counterions, namely K^+, Na^+ and NH_4^+. A detailed structure determination of Oxy-1.5 in solution in the presence of K^+ shows the same folding topology as previously reported with the same molecule in the presence of Na^+. Both conformations are symmetric dimeric quadruplexes with T_4 loops which span the diagonal of the end quartets. The stack of quartets shows only small differences in the presence of K^+ versus Na^+ counterions, but the T_4 loops adopt notably distinguishable conformations. Dynamic NMR analysis of the spectra of Oxy-1.5 in mixed Na^+/K^+ solution reveals that there are at least three K^+ binding sites. Additional experiments in the presence of NH_4^+ reveal the same topology and loop conformation as in the K^+ form and allow the direct localization of three central ions in the stack of quartets and further show that there are no specific NH_4^+ binding sites in the T_4 loop. The location of bound NH_4^+ with respect to the expected coordination sites for Na^+ binding provides a rationale for the difference observed for the structure of the T_4 loop in the Na^+ form, with respect to that observed for the K^+ and NH_4^+ forms.

INTRODUCTION

Telomeres are the specialized structures at the ends of linear chromosomes in eukaryotes and are composed of DNA and associated proteins. Telomere DNA in most species comprises tens to thousands of repeats of a short sequence in which one strand shows a bias for guanines (1–3). The G-rich strand generally has a single strand overhang of about two telomere sequence repeats. In the protozoan *Oxytricha nova*, the telomere repeat is $d(T_4G_4)$. Biochemical studies of oligonucleotides containing two or more units of the *Oxytricha* telomere sequence repeat have demonstrated that these oligonucleotides can form G-quadruplexes under appropriate conditions (4,5). An NMR (6,7) as well as an X-ray crystal structure (8) of $d(G_4T_4G_4)$ [Oxy-1.5] have been reported. In both cases, a symmetrical dimeric quadruplex with four G-quartets, *syn–anti–syn–anti* glycosidic torsion angles along each G-strand and a four thymine loop at each end of the quadruplex were observed. However, in solution the thymines loop across the diagonal of the end quartets (Fig. 1), while in the crystal structure the thymines loop across the wide grooves (7). The NMR sample was prepared in 50 mM NaCl, while the crystallization sample contained K^+ as the predominant counterion. It has been proposed that the different species of counterion could explain the difference between the solution and crystal structures (9).

Differences in the species of coordinated cation, even the ratio $[Na^+]$ versus $[K^+]$ present, have also been invoked to explain the apparent formation of multiple quadruplex conformations for the same oligonucleotide sequence as analyzed by gel electrophoresis and Raman and CD spectroscopy (10–12). In several of these studies it has been reported that associated cations can determine the type of quadruplex formed (parallel versus antiparallel, dimer versus fold-back structures) and that simultaneously present conformations are in slow exchange (of the order of hours or days) with each other.

The exceptional stability of G-quadruplexes *in vitro* and the topology of their three-dimensional structure have inspired models for a special functionality of telomere DNA sequences in chromosomes (4,5). Quadruple helical segments would be highly dissimilar from all double-stranded structural motifs and could thus easily be conceived as being crucial for control and regulation of telomerase activity. Indirect evidence for the

*To whom correspondence should be addressed. Tel: +1 310 206 6922; Fax: +1 310 825 0982; Email: feigon@mbi.ucla.edu

existence of G-quadruplexes *in vivo* comes from studies which have shown that some telomere binding proteins bind to and/or facilitate formation of G-quadruplexes (13–15). The circumstantial evidence for G-quadruplex formation at the ends of telomeres and the fact that these structures interfere with telomerase activity (16), an enzyme responsible for telomere maintenance whose hyperactivity is associated with some forms of cancers, has inspired the development of molecules which stabilize G-quartet formation (17). Some of these molecules have proven successful in limiting telomerase activity *in vitro* (18). Additionally, several *in vitro* selected oligonucleotides have been shown to form G-quadruplex structures. Examples include a two G-quartet aptamer which binds to and inhibits thrombin (19,20) and several other G-quartet-containing aptamers which inhibit cell transfection by HIV *in vitro* (21–23).

In order to provide further insight into the role of monovalent cations in G-quadruplex folding and conformation, we have investigated the solution structure of Oxy-1.5 in the presence of K^+ and NH_4^+. Although the resonance frequencies in the proton NMR spectra differ significantly for Oxy-1.5 in solutions containing K^+ and NH_4^+ compared to Na^+, the NOESY crosspeak patterns are essentially the same for all three cations. Analysis of the NOESY spectra indicates that a diagonally looped dimeric quadruplex is formed with K^+ and NH_4^+ counterions as well as with Na^+. A comparison of the refined structure of Oxy-1.5 in the K^+ form, presented here, with the previously determined Na^+ form (6,7) shows that the overall topology under both conditions is the same. However, there are some significant differences in the conformations of the two structures, primarily in the position of the bases in the thymine loops. In the presence of NH_4^+ as the counterion, the thymine loops adopt essentially the same conformation as with K^+. Dynamic NMR analysis of the spectra of Oxy-1.5 in mixed Na and K solution shows that there are at least three K^+ binding sites. This is consistent with previous analysis of NOESY spectra of Oxy-1.5 in NH_4^+, which showed that there are three NH_4^+ binding sites, one between each pair of quartets (24,25). Further analysis presented here indicates that there are no additional specific NH_4^+ binding sites in the T_4 loops. The positions of Na^+ observed in the high resolution (0.95 Å) crystal structure of the parallel tetrameric quadruplex $[d(TG_4T)]_4$ (26,27) versus the positions of the NH_4^+ within the dimeric Oxy-1.5 quadruplex (24,25) suggests a possible origin for the differences observed in the loop structures of the Na^+ form versus the K^+ and NH_4^+ forms of Oxy-1.5.

MATERIALS AND METHODS

Sample preparation

The Oxy-1.5 samples were prepared as previously described for the Na^+ structure (28) except for the last steps, where the counterion was changed to K^+. In brief, the DNA was chemically synthesized using phosphoramidite chemistry on an ABI 381A DNA synthesizer, deblocked with concentrated aqueous ammonia, precipitated with ethanol in the presence of 1 M NaCl and purified on a Sephadex G50 (Pharmacia) column. Fractions containing only full-length oligonucleotide were pooled, lyophilized and redissolved in 50 mM NaCl solution. To change the counterion to K^+, the DNA was desalted on a Sephadex G25 column and passed over a Bio-Rad AG-50 cation exchange column that had been charged with K^+. The DNA was lyophilized and stored until use. The NMR sample for the K^+ structure determination was prepared by dissolving the sample in 50 mM KCl and adjusting the pH to 6.0 using KOH. The sample concentration was 5.0 mM in strand in 450 µl of D_2O or 90% H_2O/10% D_2O. The same sample was used for both the H_2O and D_2O spectra; the solvent was exchanged by lyophilization in the NMR tube followed by redissolving the sample in 450 µl D_2O or 90% H_2O/10% D_2O. For the K^+ titration experiments, an NMR sample of Oxy-1.5 in 50 mM NaCl was prepared as described. Aliquots of concentrated KCl solutions were added, while the total sample volume was kept within 2% of the original volume by occasional drying under a stream of N_2. Ammonium ion samples were prepared by passing a purified sample of Oxy-1.5 over a Sephadex G25 column equilibrated and eluted with 1.0 mM $^{15}NH_4Cl$ and adjusting the pH with LiOH after lyophilization and resuspension as described (25). Final sample conditions were 2.5 mM Oxy-1.5 quadruplex, 55 mM in NH_4^+ at pH 5.0.

K^+ titration and dynamic NMR analysis

In an attempt to determine the number of cations bound within Oxy-1.5 a dynamic NMR analysis was preformed on spectra from a Na^+–K^+ titration experiment (Fig. 4). For this analysis the line shapes of the G12H8 resonance (~8.2 p.p.m. in the K^+ form) were fit with a two-site exchange model (29) using a least squares minimization in the data analysis software IGOR Pro (WaveMetrics, Lake Oswego, OR). This resonance was selected since it exhibits substantial line broadening over the course of the titration and is well resolved from other resonances. The resonance line shapes of G12H8 at all KCl concentrations could be modeled as a system with a single slow step undergoing two-site exchange which is intermediate on the NMR time scale. Thus, there is no evidence for more than one slow step in the conversion of Oxy-1.5 from the Na^+ to the K^+ form, but this does not rule out the possibility of additional steps which are fast on the NMR time scale. From our analysis of the G12H8 resonance, populations of the species on each side of the slow step and their effective dynamic NMR parameter τ were extracted from spectra acquired from 1 to 14 mM KCl. Models for the conversion of Oxy-1.5 from the Na^+ to the K^+ form were then tested for validity by determining if any set of rate constants existed which allowed a given model to simultaneously satisfy both the observed population and τ values. The simplest model of the Na^+ form of Oxy-1.5 being converted to the K^+ form by a single cation exchange event (i.e. a single cation binding site) was found to be inconsistent with the population values for any given rate constants. Models containing one intermediate species (a Na^+K^+ form of Oxy-1.5) were not able to fit both the population and τ values simultaneously. Thus, we were able to rule out the possibility that less than four unique species of Oxy-1.5 exist over the course of the Na^+–K^+ titration. This established the presence of at least two intermediate forms (a $Na^+{}_2K^+$ form and a $Na^+K_2^+$ form), implying at least three cation coordination sites. At the final stage of model complexity, models were tested which contained these two intermediate species. Some of these were found which simultaneously fit both the population data and τ, within experimental error. However, because of the interdependence of the rate constants and our lack of knowledge concerning the exact chemical

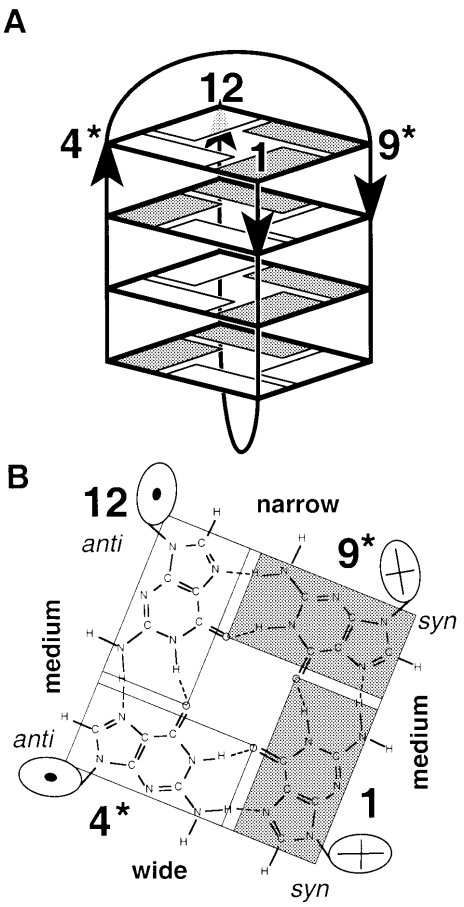

Figure 1. Schematic illustration of (**A**) the solution structure of Oxy-1.5 and (**B**) the guanine quartet at the end of the quadruplex. The strand directions are indicated by arrows. Crosses and points in the ellipses representing the deoxyribose moieties of the quartet are arrow heads and tails. The locations of the bases relative to the ribose rings are represented by the positions of the ellipses. The different types of grooves are indicated. Oligonucleotides of one strand are numbered 1–12; the symmetry related strand is numbered 1*–12*. *syn* nucleotides are shaded.

shifts of the two putative intermediate species, a unique set of values for the rate constants could not be established.

NMR spectroscopy for structure determination

NMR spectra of the K^+ form of Oxy-1.5 were acquired at the same temperatures and processed as described for the Na^+ form of Oxy-1.5 (7,28). Assignments of the K^+ form were obtained as previously described, except in this case it was not necessary to use inosine derivatives to confirm assignments (28). Spectra used to obtain nuclear Overhauser effect (NOE) and dihedral angle restraints used in the structure calculations on the K^+ form of Oxy-1.5 were four NOESY spectra acquired with mixing times of 40, 70, 100 and 140 ms, one homonuclear P.COSY spectrum, one ^1H-^{31}P heteroCOSY spectrum of the sample in D_2O at 25°C and four NOESY spectra of the same sample in 90% H_2O/10% D_2O obtained with mixing times of 25, 50, 100 and 200 ms at 5°C. NMR spectra of the NH_4^+ form

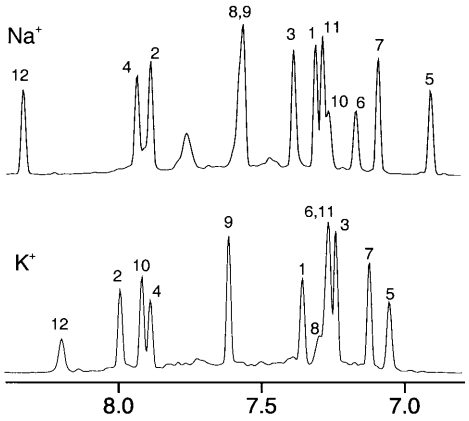

Figure 2. One-dimensional ^1H NMR spectra of the aromatic region of Oxy-1.5 in D_2O at 5 mM strand concentration and pH 6.0 in (top) 50 mM NaCl at 20°C and (bottom) 50 mM KCl at 25°C. Assignments of the aromatic proton (GH8 and TH6) resonances of specific nucleotides are indicated.

of Oxy-1.5 were acquired and processed and assignments were made as described (25).

Structure calculations

Procedures to quantify NOE information for structure calculations were kept as close as possible to the case of the Na^+ form structure and are described in brief below. NOE crosspeaks were integrated using AURELIA. The integrated peak intensities obtained from NOESY experiments in D_2O at 70 ms and in H_2O at 100 ms were used to derive upper distance limits. The most intense H2'–H2" crosspeaks in each spectrum was equated with a distance of 1.9 Å and all remaining intensities were converted to upper distance bounds using the $I \sim r^{-6}$ relation. To account for errors in the peak integration and inherent in the two-spin approximation, a margin of 0.5 Å was added to all bounds obtained from D_2O spectra. Distances involving exchangeable protons were used with a margin of 1.5 Å to account for the greater uncertainty of some of these peak intensities. A total of 293 distance restraints, of which 54 involved exchangeable protons, were obtained, corresponding to an average of 24 crosspeaks per nucleotide. This constitutes 80% of the corresponding numbers obtained for the Na^+ form of Oxy-1.5. The smaller number of unambiguously assigned NOE crosspeaks for the K^+ form of Oxy-1.5 is mainly caused by greater peak overlap compared to the Na^+ form spectra, which therefore meant that fewer crosspeak intensities could be quantified for the structure calculations. All constraints were duplicated for the symmetry equivalent proton pairs. In each G-quartet, all of the eight hydrogen bonds were restrained to standard hydrogen bond distances of 1.9 Å. The structures were calculated with X-PLOR v.3.1. Since only one set of signals was observed for each nucleotide, symmetry was assumed and enforced in the calculations as previously described.

Coupling constants H1'–H2', H1'–H2", H2'–H3' and H2"–H3' were determined from P.COSY spectra by an automatic optimization of the correlation between experimental and simulated data points covering the relevant crosspeaks using the program CHEOPS (P.Schultze and J.Feigon, unpublished).

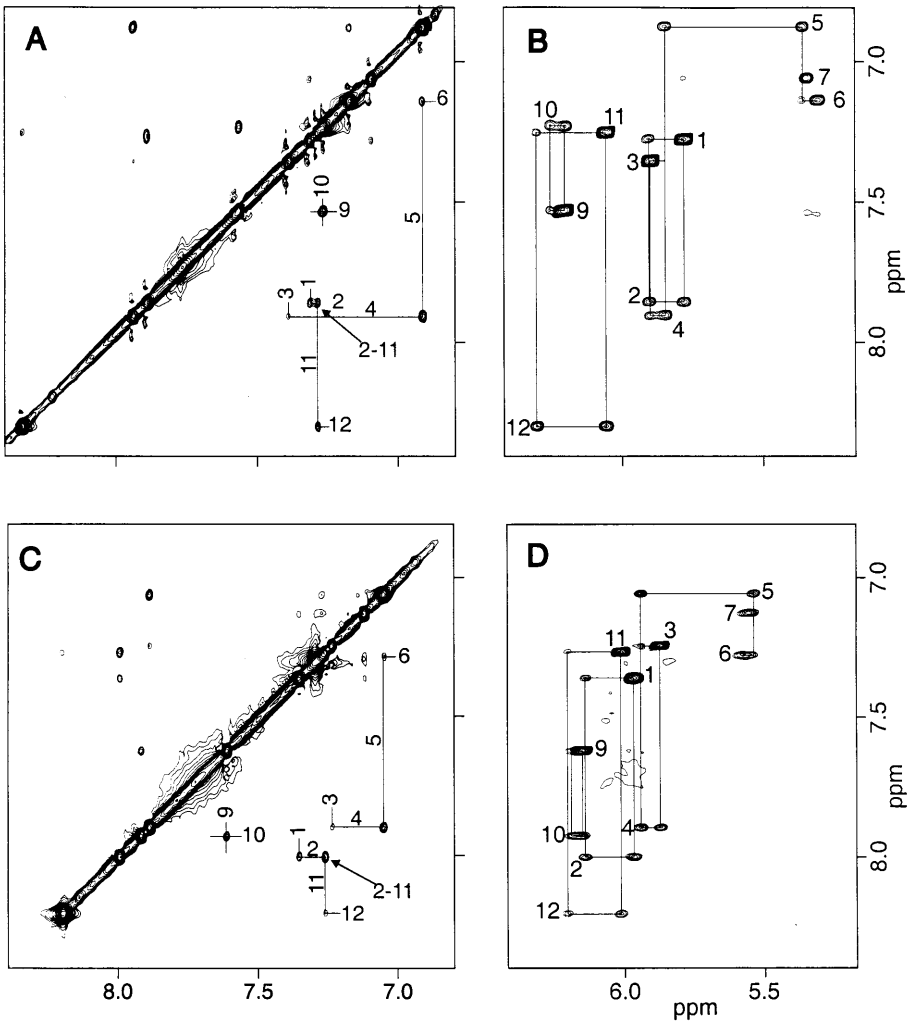

Figure 3. Portions of the NOESY spectra of Oxy-1.5 in 50 mM NaCl showing (**A**) the aromatic–aromatic and (**B**) aromatic–H1' regions. Equivalent spectral regions in the presence of 50 mM KCl are shown in (**C**) and (**D**). Sample conditions are as in Figure 2. Inter-residue aromatic–aromatic (A and C) and sequential aromatic–H1' (B and D) crosspeaks are labeled. The spectra were processed with 600 complex points in T2 and 323 (Na^+ form) and 424 (K^+ form) complex points in T1 and were zero filled to 2K points in both dimensions. A squared sine bell apodization function with a shift of 60° and a skew factor of 1.1 was applied in both dimensions.

The deoxyribose sugar conformations were calculated using these coupling constants as input for the PSEUROT program (30), as previously described. In the structure calculations, the ribose conformations were restrained to their major forms, which was in all cases an S-type conformation, just as for the Na^+ form of Oxy-1.5.

In contrast to the Na^+ form of Oxy-1.5, we were unable to use a ^1H-^{31}P heteroCOSY spectrum to estimate the coupling constants $J_{H5',P}$, $J_{H5'',P}$ and $J_{H3',P}$ due to spectral overlap. Therefore, no restraints were obtained for the backbone angles β and ε. The γ angle for all *anti* nucleotides was restrained to 60 ± 40° as previously described. To enforce correct configurations at the chiral centers an additional set of dihedral angle restraints involving all four ligands on each chiral center was introduced throughout all calculations in the same way as for the Na^+ form of Oxy-1.5 (31).

To ensure comparability between the Na^+ and the K^+ forms of Oxy-1.5, all X-PLOR protocols used were taken from the versions for the Na^+ form and used with identical parameters except for the new distance and dihedral restraint files. The sequence of calculations involved the four steps: (i) substructure embedding using the metric matrix distance geometry algorithm; (ii) completion of the partial coordinate sets by template fitting and regularization of this initial set of embedded structures by simulated annealing; (iii) refinement of the best converged structures by simulated annealing and minimization; and (iv) relaxation matrix refinement. For the final relaxation matrix refinement, a grid search for the correlation time that would give the best agreement between calculated and observed NOE intensities for the 4×432 peak integrals from the four D_2O NOESY spectra was performed using the coordinates of the lowest energy structure from step 3. This gave an overall

correlation time of 8.5 ns, which was used for all relaxation matrix refinement. The relaxation matrix refinement protocol resulted in a significant drop in the *R* factor between observed and calculated peak integrals from around 0.12 to 0.08.

Coordinates for the eight lowest energy structures of Oxy-1.5 in K^+ have been deposited in the RCSB Protein Data Bank (accession number 1k4x).

RESULTS AND DISCUSSION

Comparison of ^{1}H NMR spectra of Oxy-1.5 in Na^+ and K^+

One-dimensional spectra of the aromatic region of Oxy-1.5 in 50 mM NaCl and in 50 mM KCl are shown in Figure 2. Large chemical shift changes are observed for many of the resonances, the largest being the thymine residues and G10. In contrast, the crosspeak patterns and intensities for most of the residues of Oxy-1.5 in K^+ are the same as for Oxy-1.5 in Na^+. For comparison, portions of NOESY spectra of Oxy-1.5 in K^+ and in Na^+ are shown in Figure 3. For both the Na^+ and K^+ samples, half of the guanines exhibit the strong GH8–H1' NOEs indicative of the *syn* conformation and the same patterns of NOE connectivities between 5'-G*syn*–G*anti*-3' steps are observed (Fig. 3B). For each 5'-*syn*–*anti*-3' guanine pair there is a sequential G_nH8–$G_{n+1}H8$ crosspeak. In addition, there is one long-range (non-sequential) connectivity between G2H8 and G11H8 (Fig. 3A). The only end-looped symmetrical dimeric quadruplex of Oxy-1.5 in which G2H8 and G11H8 are within NOE distance of each other is the diagonally looped structure previously reported for Oxy-1.5 in Na^+ (28). In contrast, for the edge-looped structure found in the crystal, there would be no non-sequential *syn–anti* H8–H8 connectivities at all, as both the intra-quartet and inter-quartet G2H8 and G11H8 distances are >6 Å. In tetrameric quadruplexes with parallel strands *syn* bases have not been observed. Thus, qualitative analysis of the NOESY spectra indicates that Oxy-1.5 adopts the same folded (diagonally looped) topology in both Na^+- and K^+-containing solutions.

Oxy-1.5 has at least three K^+ binding sites

Figure 4 shows the one-dimensional ^{1}H NMR spectra of Oxy-1.5 in a titration experiment in which increasing amounts of KCl were added to an Oxy-1.5 sample originally containing 50 mM Na^+. As the KCl was added the proton spectra gradually converted from the Na^+ form to the K^+ form spectrum, with a number of resonances moving monotonically from their Na^+ to their K^+ form chemical shift. However, at a K^+ concentration between ~1 and 10 mM significant line broadening is observed for several proton resonances (Fig. 4). This indicates intermediate exchange kinetics on the NMR chemical shift time scale (i.e. in the millisecond range). The resonances narrow again as the concentration of KCl is increased to >10 mM. We previously reported a similar titration experiment of the three-quartet dimeric quadruplex formed by $d(G_3T_4G_3)$ (32). For this three quartet quadruplex almost no line broadening is observed, but the fast exchange kinetics of coordinated cations also led to a characteristic movement of proton resonance frequencies over the course of the titration. This movement of chemical shifts as a function of K^+ concentration was found to be perfectly consistent with one intermediate species, in addition to the pure Na^+ and pure K^+ forms of $[d(G_3T_4G_3)]_2$. This intermediate is presumably the mixed Na^+-K^+ form of $[d(G_3T_4G_3)]_2$, i.e. $[d(G_3T_4G_3)]_2$ coordinating

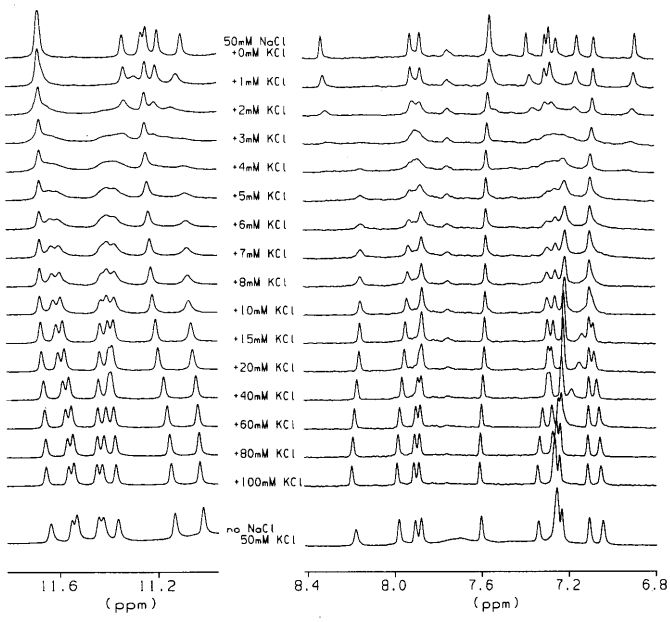

Figure 4. A series of one-dimensional spectra of Oxy-1.5 at 25°C, 5 mM strand, pH 6.0 in 50 mM NaCl plus increasing amounts of KCl (from 0–100 mM). Spectral regions of imino (left) and aromatic proton resonances (right) are shown with salt concentrations indicated between the p.p.m. ranges. The spectrum at the bottom is of a sample in 50 mM KCl and no NaCl.

one Na^+ and one K^+. Thus, it was concluded that the $[d(G_3T_4G_3)]_2$-quadruplex contains two cation coordination sites presumably existing between each pair of stacked G-quartets. Furthermore, this analysis resulted in determination of the equilibrium constants for conversion of the Na^+ to the K^+ form and thus the relative affinity of $[d(G_3T_4G_3)]_2$ for Na^+ versus K^+.

Here we have applied the same chemical shift analysis that was successful in determining the number of cations bound to $[d(G_3T_4G_3)]_2$ to the titration data for $[d(G_4T_4G_4)]_2$. In addition, we performed a dynamic NMR analysis in which line shapes predicted by various kinetic models were fitted to the resonances which exhibited appreciable broadening during the titration (Materials and Methods). This analysis revealed that *at least two intermediate species are required for any model to be consistent with the titration data, which means that there are at least three cation binding sites.* Due to the lack of knowledge concerning the chemical shifts of the intermediate species a unique solution for the equilibrium constants for these species could not be determined. In the case of $[d(G_3T_4G_3)]_2$ this problem was tractable since there was only one intermediate species of unknown chemical shift. Without the equilibrium constants for the different forms of $[d(G_4T_4G_4)]_2$ it was not possible to determine the exchange rates between these forms using the line broadening data, since such a determination requires knowledge of the relative populations and chemical shifts of the intermediate species (29). Nevertheless, we are able to conclude that at least two intermediate species exist during the course of the titration from the Na^+ to the K^+ form of Oxy-1.5, consistent with there being three cation coordination sites within Oxy-1.5 which can coordinate

cations with a stoichiometry of Na^+_3, $Na^+_2K^+$, $Na^+K^+_2$ or K^+_3 over the course of the titration. These results are in contrast to the observation of only a single diffuse ion in the crystal structure of Oxy-1.5 (8).

Solution structure of Oxy-1.5 with K^+

The three-dimensional structure of the K^+ form of Oxy-1.5 was calculated with metric matrix distance geometry starting structures and refined by simulated annealing using slightly modified X-PLOR protocols (33). The eight lowest energy structures were then further refined by direct NOE refinement. In order to be able to directly compare this structure with the previously reported structure of the Na^+ form of Oxy-1.5 (7), the processing of the NMR data and the structure calculations were carried out using identical protocols for the two different structures. The distance restraints used in the structure calculations are summarized in Table 1. The total number of distance restraints per oligonucleotide strand is 293, of which 160 are inter-residue and 54 involve exchangeable protons. There are also 54 dihedral angle restraints per strand. The final structures before relaxation matrix refinement contained no distance violations >0.5 Å and no dihedral angle violations >5°. The refinement statistics are given in Table 2.

Table 1. NMR-derived distance restraints used in the structure calculations of the Na^+ and K^+ forms of Oxy-1.5

	K^+	Na^+
Total	293	359
Intranucleotide	160	135
Internucleotide	133	224
Exchangeable	54	59
Torsion angle	27	28

Table 2. Refinement statistics for the K^+ form of Oxy-1.5

NOE violations >0.5 Å	0
Dihedral angle violations >5°	0
Average r.m.s.d. from ideal covalent geometry	
Bond lengths (Å)	0.022
Bond angles (°)	6.6
Relaxation matrix refinement	
Number of peak integrals at each mixing time	432
Average $R^{1/6}$ factor before	0.1212 ± 0.0011
Average $R^{1/6}$ factor after	0.0793 ± 0.0009

Stereo views of the eight best (i.e. lowest energy) structures of the K^+ form of Oxy-1.5 are shown in Figure 5. Most of the residues are well defined, giving an overall root mean square deviation (r.m.s.d.) of 1.09 Å for the ensemble of structures shown (Table 3). As is the case for the Na^+ form, the K^+ form of Oxy-1.5 is a dimeric quadruplex in solution with alternating *syn* and *anti* nucleotides along each G_4 segment and T_4 loops which cross the diagonal of the end G-quartets (Fig. 1). There

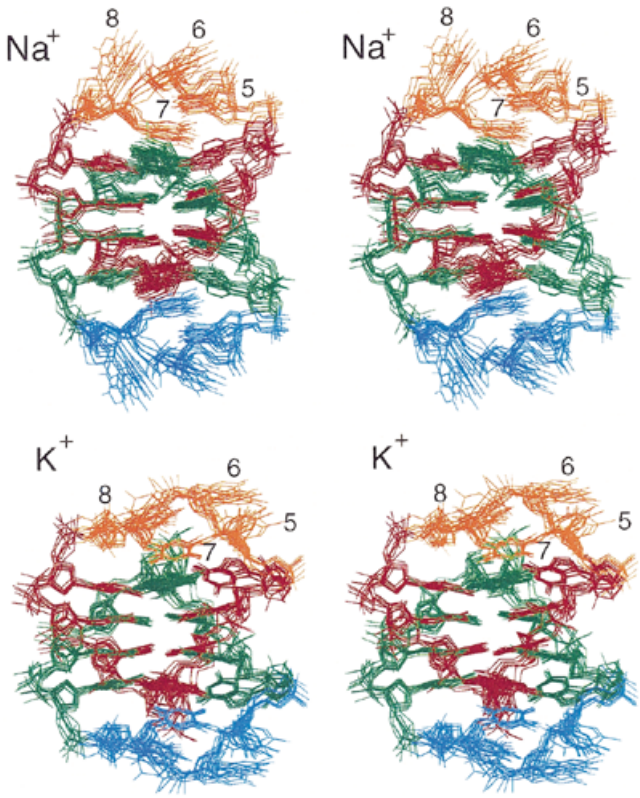

Figure 5. Stereo views of an ensemble of eight structures each of the Na^+ (top) and K^+ (bottom) forms of Oxy-1.5. Residue numbers are shown for one T_4 loop. The symmetry equivalent strands are distinguished by red versus green color for G residues and orange versus blue for the T_4 loops.

are three different groove widths; one narrow groove, two medium grooves and one wide groove.

Table 3. Average r.m.s.d. (Å) of the ensemble of eight lowest energy structures of the Na^+ and K^+ forms of Oxy-1.5 and cross-r.m.s.d. for the two forms

	All residues	G-quartets	T loops
Na^+	0.94	0.81	0.66
K^+	1.04	0.97	0.84
Cross	2.38	1.62	2.17

Comparison of the Na^+ and K^+ forms of Oxy-1.5

Although the overall fold of the Na^+ and K^+ forms of Oxy-1.5 are the same, there are some visible differences between the two structures (Fig. 5), especially in the T_4 loop (Fig. 6). In order to assess the significance of the differences between the Na^+ and K^+ forms of Oxy-1.5, we first compared the conformational variability between the two forms to the variability within the conformational ensembles of each form. The overall r.m.s.d. for all heavy atoms in each of the two ensembles of structures is ~1 Å, but the r.m.s.d. between the two ensembles is significantly

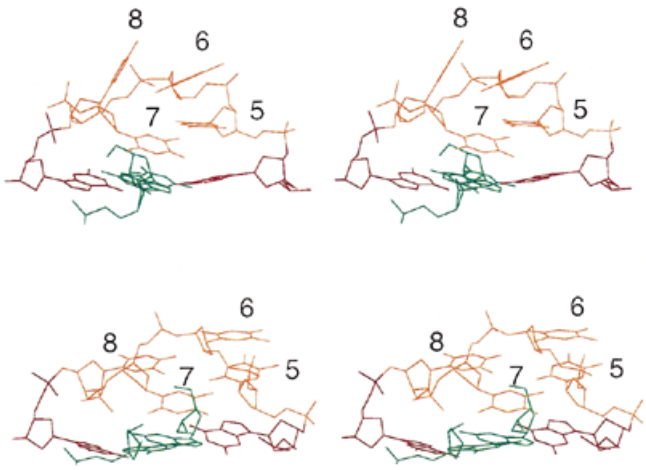

Figure 6. Stereo view of the top G-quartet and T_4 loops of a superimposition of the lowest overall energy structures of the Na^+ (top) and K^+ (bottom) forms. To emphasize the differences in loop conformation only the guanine residues were used for the superimposition. The color scheme is as in Figure 5.

greater at 2.38 Å (Table 3). The average for the K^+ form is slightly greater than for the Na^+ form, which is expected due to the lower number of restraints available compared to the Na^+ form. However, it is still significantly smaller than the cross average. If only the guanine nucleotides are used, the r.m.s.d. difference is 1.42 Å. However, the thymine loops alone show a much larger r.m.s.d. difference of 2.17 Å (Table 3).

The results of the structure refinements depend on the set of distance restraints used. Thus, it could be argued that the differences between the two sets of restraints might be caused by errors in peak assignments or missed contacts because of peak overlap in the two cases. To address this point, two methods of checking were used. Initially, a list of all NOEs involving loop residues obtained from the Na^+ spectra was manually checked to determine which of the analogous peaks also occurred in the K^+ form data. It was found that crucial peaks present in the Na^+ form do not occur in the K^+ form. Furthermore, after structure refinement, distance violations of the Na^+ form with respect to the K^+ restraints (and vice versa) were calculated and the corresponding peak assignments were rechecked in the corresponding spectra.

The differences between the conformation of the thymine loops in the two structures can clearly be seen in the structures (Fig. 6). In the Na^+ form of Oxy-1.5, T5 stacks over the center of the G4·G12* base pair (* refers to the symmetry related strand), T6 stacks on T5, T7 folds down to stack over the top quartet near G1*O6 with its carbonyl oxygen in close proximity to the center of the quartet and T8 is the least well constrained of all of the thymines in the loop but is usually tilted toward the O2 of T6. In the K^+ form of Oxy-1.5, T5 and T6 are also stacked on each other, but T5 is displaced outward to stack over the deoxyribose of G4. T7 is stacked over the center of the top quartet in a position somewhat displaced compared to the Na^+ form and T8 is loosely stacked on the top G-quartet, near G12*O6 at the level between T5 and T6. Overall, the thymine loop in the K^+ form appears less extended than in the Na^+ form, with T8 tucked in next to the terminal quartet rather than extended towards the solution.

The differences between the guanine quadruplex cores of the two forms of Oxy-1.5 are smaller and less obvious. We calculated the twists and rise values between quartets and out-of-plane deviation angles for the guanine bases (Table 4) and compared them for the two structures (7) and also to the crystal structure (8). The two solution structures have almost the same twist values (within 3°) for each quartet and differ significantly from the crystal structure. The out-of-plane deviation angles for the bases are small for the two inner quartets (6–15°) and within a few degrees of each other in the two structures. The base tilts for the outer two quartets are larger, but only G4 is significantly different between the two structures, with a value of 32° for the K^+ form in contrast to 18° for the Na^+ form, which is near the average for the rest of the bases in the outer quartets of the two structures. Relatively large differences are found in the rise values for the two structures. The biggest difference is for the average rise between the second and third quartets, which is 3.0 Å for the K^+ form and 3.6 Å for the Na^+ form. Under the assumption that ions are located in the center between two quartets this appears somewhat counterintuitive, given that the radius of K^+ would clearly be greater. It is, however, difficult to access the significance of the difference in rise between guanine quartets in the Na^+ and K^+ forms of Oxy-1.5, since this would be one of the least reliable parameters obtained in the solution structures. The reason for potential inaccuracy in the rise is that the NOE distance constraints are only slightly affected by variation in rise. It is a fundamental problem of DNA NMR structure calculation that sequential base distance constraints can be satisfied by variation of either stacked base spacing or helical twist. Thus, increased twist pulls the quartets together while maintaining most NOE distances constant in a nominal range. Alternatively, the difference observed in the quartet stacks could be real and result from the different nature of Na^+ and K^+ coordination by Oxy-1.5.

Table 4. Average geometric parameters for the G-quartets in the eight lowest energy structures of Oxy-1.5 (K^+ form)

Quartet[a]	Twist (°)[b]	Rise (Å)[b]	Out-of-plane deviation (°)[c]
1,4*,12,9*	16	3.2	15,32,16,18
2,3*,11,10*	36	3.0	13,13,10,9
3,2*,10,11*	23	3.2	13,13,9,10

[a]Designated by sequence numbers of G residues. Symmetry equivalent residues are marked by an *.
[b]Values refer to the step between this and the following quartet. Measured as described by Schultze *et al*. (7).
[c]Angles are given in the order of G residues in the left column.

The average backbone dihedral angles, the χ angles and the pseudorotation angles for both the Na^+ and K^+ forms of Oxy-1.5 are shown in the circle plots of Figure 7. Relatively large differences in the backbone angles of the Na^+ and K^+ forms are found primarily in the thymines, especially T6 and T8. χ and P angles for almost all residues are essentially the same for the identical nucleotides in both structures.

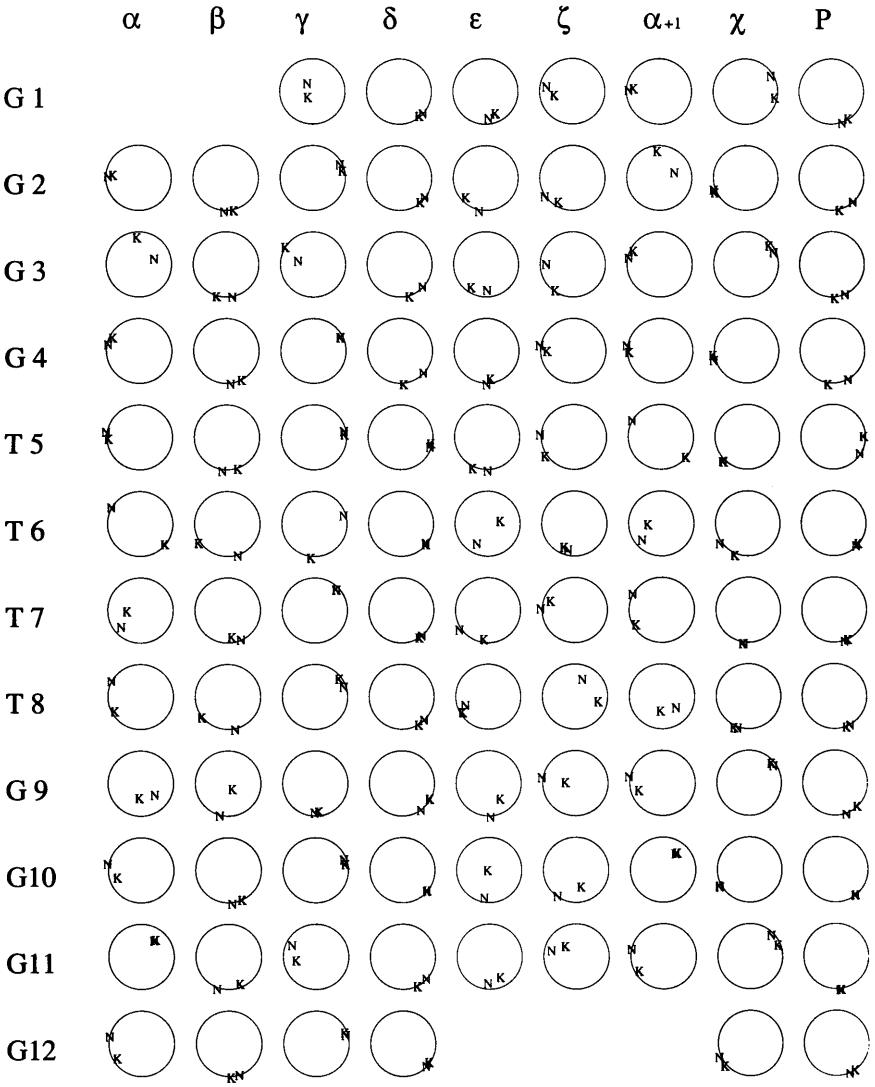

Figure 7. Circle plots of the average dihedral angles of the eight lowest energy structures of the K^+ and Na^+ forms, marked by K and N, respectively. Each value plotted represents the geometric average of the individual angles. A small distance from the center thus reflects a large degree of scatter of the angles.

Specific Na^+, K^+ and NH_4^+ coordination by Oxy-1.5

Because all of the experimental conditions other than counterion species are identical in the experiments for the Na^+ and K^+ forms of Oxy-1.5, *bona fide* differences between the two structures must arise from DNA–cation interactions. Due to the aromatic ring systems in the G-quartets, small changes in the positions of the bases or spacing between two quartets could give rise to large chemical shift changes. It has been known for many years that G-quartets coordinate specific monovalent and divalent cations tightly (4). The smaller Na^+ cation was proposed to bind in the center of a G-quartet, while the larger K^+ was thought to be restricted to binding between two quartets (34,35), in both cases via coordination with the carbonyl oxygen lone pair electrons. In a high resolution crystal structure containing end-to-end dimers of the parallel tetrameric quadruplex formed by $d(TG_4T)_4$, seven Na^+ ions were observed (26,27). They occupy a continuum of sites ranging from precisely within the plane of one G-quartet to the exact center between the planes of two G-quartets. The lower resolution crystal structure of Oxy-1.5 shows diffuse density between the two central G-quartets, which has been attributed to a single K^+ binding site (8).

In order to more specifically localize cation binding sites for Oxy-1.5 in solution, we have previously used $^{15}NH_4^+$ as a chemical probe (24,25). These experiments showed unambiguously that Oxy-1.5 binds three ammonium ions, consistent with the minimum number of K^+ binding sites determined by the dynamic NMR analysis, discussed above. The exchange of these bound ions with free ammonium in the solvent, as well as the exchange of their protons with solvent protons, is slow on the NMR time scale. Three different resonances are detected, one from bulk ammonium and two from bound ions. Of the

two bound ammonium ion resonances, the one assigned to the two symmetry equivalent 'outer' positions is twice the intensity of that from the single centrally bound ion. Relative NOE crosspeak intensities indicate that each bound ammonium ion is located in the geometric center of the eight imino protons of the pair of quartets surrounding it.

A comparison of the NOESY spectra of Oxy-1.5 with K^+ and NH_4^+ shows that the NOESY crosspeak patterns and intensities with these two counterions are very similar to one another. The K^+ and NH_4^+ forms also show the same differences in the NOEs to the loop residues when compared to the spectra of the Na^+ form. A similar coordination for NH_4^+ and K^+ would be expected on the basis of their similar van der Waals radii.

The dynamic NMR analysis of K^+ binding to Oxy-1.5 could not distinguish between three, or more than three, cation binding sites. In order to investigate the possibility that cations are also coordinated by the thymine loops of Oxy-1.5 and that a change in the species of loop-bound cation might be responsible for the observed differences in loop structure, we examined NOESY spectra for evidence of an additional ammonium ion binding site in the loops. The previously reported analysis of ammonium ion binding to Oxy-1.5 clearly showed only two resonances (intensity ratio 2:1) at chemical shifts distinct from the bulk ammonium resonance. These corresponded to three cations (two in symmetry equivalent sites) in slow exchange on the NMR chemical shift time scale. However, if there was an ammonium ion binding site in the T_4 loop that exchanged on the nanosecond time scale, no distinct ammonium ion resonance for this ion would be observed. Rather, in this fast exchange regime there would be NOE crosspeaks between the thymine resonances and the bulk ammonium ion. We have recently shown that it is possible to identify ammonium ion binding sites under such conditions of fast exchange on DNA duplexes (36). However, for Oxy-1.5 no NOE crosspeaks between any resonances in the T_4 loop and the bulk ammonium resonance are observed. We therefore conclude that there are no specific ammonium ion binding sites in the T_4 loops.

Although no ammonium ion binding sites were found in the loops of Oxy-1.5, a single NOE crosspeak between the resonance from the 'outer' ammonium ion (i.e. bound between the outer two G-quartets) and the T8 methyl protons of Oxy-1.5 is observed (Fig. 8). The origin of this crosspeak from the assigned 'outer' ammonium ion resonance was unequivocally verified in a control experiment without ^{15}N decoupling of the $^{15}NH_4^+$, in which it shows the expected splitting of ~75 Hz of the $^{15}NH_4^+$ proton resonances. Indirect magnetization transfer (i.e. spin diffusion) between the protons of this ammonium ion and the T8 methyl protons was ruled out by an additional ROESY spectrum (data not shown). Since the position of the T8 methyl is directly above the outer quartet, the simplest explanation for the origin of this crosspeak is direct transfer of an NOE from the ammonium ion bound between the outer two G-quartets to the T8 methyl. This ammonium ion–T8 methyl NOE provides an additional constraint on the position of T8 in the structure, as discussed below.

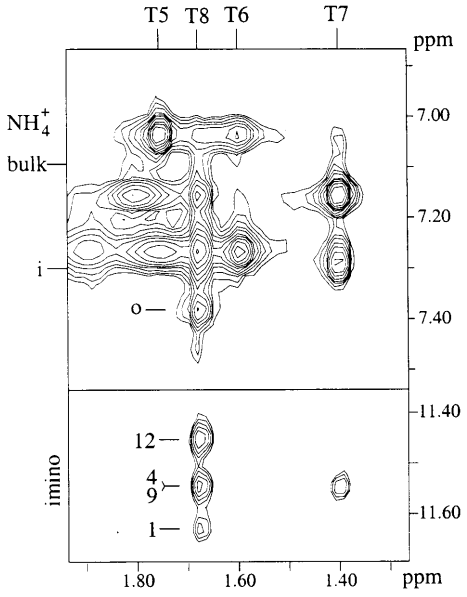

Figure 8. Regions of a NOESY spectrum of Oxy-1.5 in 95% H_2O/5% D_2O at 5.0 mM strand, 55 mM $^{15}NH_4^+$, pH 5.5 and 15°C. Suppression of the water signal was achieved by WATERGATE (41) and ^{15}N decoupling was applied in both dimensions. Regions of crosspeaks between methyl groups and ammonium protons (top) and G imino protons (bottom) are shown. Proton resonance frequencies for the bulk, inner (i) and outer (o) ammonium ions are indicated. Methyl and imino proton shifts are labeled by residue numbers.

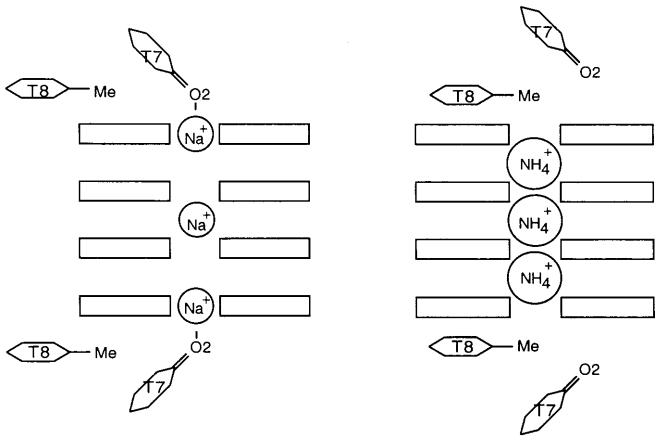

Figure 9. Scheme for proposed explanation of the differences in loop conformations caused by different ionic radii and coordination geometries. The smaller Na^+ ion (left) fits in the center of the top quartet and is coordinated by the O2 of T7. The larger ammonium ions remain in the central positions between quartets, so that T7 is no longer needed for coordination. This makes room for closer stacking of T8 on G9, which leads to the observed NOE contact to the outer ammonium ion.

A model for the difference in loop structure in Na^+ versus K^+ forms of Oxy-1.5

The lack of evidence for any T_4 loop-bound cations, taken together with the coordination geometry for Na^+ observed in the crystal structure, suggests a model for the source of the differing loop conformation observed for the Na^+ and K^+ forms of Oxy-1.5 (Fig. 9). In the case of K^+ (and NH_4^+) binding, the outer K^+ (or NH_4^+) would be located exactly between the planes of the two outer quartets. In the K^+ form of Oxy-1.5, T8 stacks directly on G9, which leaves its methyl group above and

near the center of the top quartet. NOEs are observed between the T8 methyl group and the imino protons of the top G-quartet. A similar position of T8 in the NH_4^+ form gives rise to the observed additional NOE with the ammonium ion (Fig. 8). In the case of the Na^+ form, the outer Na^+ ions would be coordinated within, or close to, the plane of the end quartets, as in the crystal structure of $[d(TG_4T)]_4$ (26). This allows for a decrease in cation–cation repulsion and for the coordination of an additional oxygen atom situated above the center of the end quartet, as is furnished by the water molecule observed in the crystal structure of $[d(TG_4T)]_4$. In the NMR structure of the Na^+ form we find that, even without using any explicit cations in the structure calculations, the O2 atom of T7 is close to the geometric center of the top quartet at a distance of ~3.6 Å. We hypothesize that T7 is positioned to allow binding of T7O2 to the Na^+ ion, in analogy to the Na^+-bound water molecule observed in the crystal structure of $[d(TG_4T)]_4$. This displaces T8 from the central well-stacked position seen in the K^+ (and NH_4^+) form of Oxy-1.5.

Comparison with Na^+ and K^+ forms of $[d(G_3T_4G_3)]_2$ and $[d(G_3CT_4G_3C)]_2$

A recent report has compared the conformational differences between the Na^+ and K^+ forms of $[d(G_3T_4G_3)]_2$ (37), which forms an asymmetric quadruplex with three stacked G-quartets and diagonal loops like Oxy-1.5 (32,38). As with Oxy-1.5, the topology of the quadruplex did not change upon conversion from the Na^+ to the K^+ form (32) and the loops of $[d(G_3T_4G_3)]_2$ exhibited the largest cation-dependent structural change. A qualitative comparison of the solution structure for Oxy-1.5 (7) with that of $[d(G_3T_4G_3)]_2$ in the presence of Na^+ (39) reveals that the loop structures determined for these two molecules are the same within experimental error. For the K^+ form, however, Strahan *et al*. (37) use molecular modeling evidence to argue that the loops of $[d(G_3T_4G_3)]_2$ in K^+ are in exchange between two dominant conformations, with the most distinctive difference being the stacking of T7 on the end G-quartet in the minority conformation (23% for both loops) and the unstacking of this base in the major conformation (77% for both loops). We note that Oxy-1.5 has two symmetrical loops, while in the asymmetric $[d(G_3T_4G_3)]_2$ the two loops are not strictly equivalent. The loop equivalent to that in Oxy-1.5 (crossing the diagonal of the two quartets with head-to-head stacking; 38) is in the minority conformation 9% and the majority conformation 91% of the time. This thymine base (T7) is equivalent to T8 and T8* in Oxy-1.5. Our structure determination did not result in any evidence of two distinct positions for this thymine base. We do observe the line broadening of proton resonances of this base that Strahan *et al*. (37) have presented as evidence of a dynamic equilibrium between two loop structures. However, the relatively strong NOE crosspeak between the T8 methyl protons and the ammonium ion coordinated between each of the outer and inner quartets of Oxy-1.5 (Fig. 8) would not be observed if the stacked T8 conformation is a minor conformation of only a few percent in the NH_4^+ form and, equivalently, in the K^+ form of Oxy-1.5. Thus, the T_4 loop in the K^+ form of Oxy-1.5 most closely resembles the minor loop conformation reported by Strahan *et al*. (37).

The dimeric quadruplex formed by the oligonucleotide $d(GGGCT_4GGGC)$ also shows Na^+ and K^+ forms which are in slow exchange on the NMR time scale (40). Conformational changes associated with this change in coordinated cation involve both alterations in loop and quartet structure. Interestingly, T7 in the Na^+ form of this quadruplex also points down toward the center of the end quartet and it is suggested that it participates in coordination of the Na^+. The authors propose that a K^+ binding site in the loop accounts for the structural change in the loop from the Na^+ to the K^+ form. How relevant these loop structures are to those of Oxy-1.5 is not obvious, since $d(GGGCT_4GGGC)$ forms a dimeric edge-looped (as opposed to a diagonal loop) topology with mixed G·C·G·C quartets stacked on the outside of two stacked G-quartets. Nevertheless, these structures provide another important example of cation-specific conformational changes that can occur in nucleic acids.

CONCLUSIONS

Oxy-1.5, as well as other DNA sequences containing two or more G-tracts, readily forms quadruplexes under physiological salt conditions. We report the result of a structure determination by NMR in solution in the presence of K^+ ions. A comparison of this structure with the previously determined conformation with Na^+ counterions shows that both possess the same folding topology and similar stacked G-quartet geometry but display a notable difference in the conformation of the diagonal T_4 connecting loops.

Dynamic NMR analysis of Oxy-1.5 in mixed Na^+ and K^+ solutions indicated that there are at least three K^+ binding sites in Oxy-1.5. Three binding sites were also detected for ammonium ions, in which case it was possible to directly observe NOE contacts between the centrally coordinated ions and protons of Oxy-1.5. This provides unambiguous information about the number and coordination geometry of the monovalent cations that are necessary to form G-quadruplex DNA. No additional specific binding sites of NH_4^+, and by analogy K^+, in the T_4 loops were detected, even under conditions of fast exchange (nanosecond time scale).

The direct NOE crosspeaks between a T methyl group of Oxy-1.5 with a bound ammonium ion reported here provided an additional constraint for determination of the loop conformation. The lack of a crosspeak between the same methyl group and imino protons of the end G-quartet in the Na^+ form has led us to the hypothesis that the loop conformation in the case of bound Na^+ might be controlled by coordination of a sodium ion located within the plane of the outer quartets with a carbonyl oxygen of a loop T residue. Thus, for nucleic acid molecules in general which contain G-quartets, the ammonium cation provides a valuable tool for identification of resonances from imino protons belonging to adjacent G-quartets and for additional constraints to bases closely associated with these quartets. In structures only suspected of containing G-quartets, as is the case with many G-rich *in vitro* selected nucleic acids, observation of tightly bound NH_4^+ ions would provide a valuable confirmation for the presence of stacked G-quartets.

The observation that both conformations with Na^+ and K^+ are not topologically different argues against the difference in ionic conditions as an explanation for the difference between the solution and crystal structures of Oxy-1.5.

ACKNOWLEDGEMENTS

The authors thank F. A. L. Anet for assistance with the dynamic NMR analysis. This work was supported by NIH grant GM48123 to J.F.

REFERENCES

1. Blackburn,E.H. (1990) *J. Biol. Chem.*, **265**, 5919–5921.
2. Blackburn,E.H. (1991) *Nature*, **350**, 569–573.
3. Zakian,V.A. (1989) *Annu. Rev. Genet.*, **23**, 579–604.
4. Williamson,J.R. (1994) *Annu. Rev. Biophys. Biomol. Struct.*, **23**, 703–730.
5. Williamson,J.R., Raghuraman,M.K. and Cech,T.R. (1989) *Cell*, **59**, 871–880.
6. Smith,F.W. and Feigon,J. (1992) *Nature*, **356**, 164–168.
7. Schultze,P., Smith,F.W. and Feigon,J. (1994) *Structure*, **2**, 221–233.
8. Kang,C., Zhang,X., Ratliff,R., Moyzis,R. and Rich,A. (1992) *Nature*, **356**, 126–131.
9. Frank-Kamenetskii,M.D. (1992) *Nature*, **356**, 105.
10. Sen,D. and Gilbert,W. (1990) *Nature*, **344**, 364–366.
11. Hardin,C.C., Henderson,E., Watson,T. and Prosser,J.K. (1991) *Biochemistry*, **30**, 4460–4472.
12. Miura,T., Benevides,J.M. and Thomas,G.J.,Jr (1995) *J. Mol. Biol.*, **248**, 233–238.
13. Fang,G. and Cech,T.R. (1993) *Biochemistry*, **32**, 11646–11657.
14. Fang,G. and Cech,T.R. (1993) *Cell*, **74**, 875–885.
15. Giraldo,R. and Rhodes,D. (1994) *EMBO J.*, **13**, 2411–2420.
16. Zahler,A.M., Williamson,J.R., Cech,T.R. and Prescott,D.M. (1991) *Nature*, **350**, 718–720.
17. Borman,S. (1998) *Chem. Eng. News*, **76**, 42–46.
18. Fedoroff,O.Y., Salazar,M., Han,H., Chemeris,V.V., Kerwin,S.M. and Hurley,L.H. (1998) *Biochemistry*, **37**, 12367–12374.
19. Macaya,R.F., Schultze,P., Smith,F.W., Roe,J.A. and Feigon,J. (1993) *Proc. Natl Acad. Sci. USA*, **90**, 3745–3749.
20. Wang,K.Y., McCurdy,S.N., Shea,R.G., Swaminathan,S. and Bolton,P.H. (1993) *Biochemistry*, **32**, 1899–1904.
21. Mazumder,A., Neamati,N., Ojwang,J.O., Sunder,S., Rando,R.F. and Pommier,Y. (1996) *Biochemistry*, **35**, 13762–13771.
22. Wyatt,J.R., Vickers,T.A., Roberson,J.L., Buckheit,R.W., Klimkait,T., Debaets,E., Davis,P.W., Rayner,B., Imbach,J.L. and Ecker,D.J. (1994) *Proc. Natl Acad. Sci. USA*, **91**, 1356–1360.
23. Jing,N.J. and Hogan,M.E. (1998) *J. Biol. Chem.*, **273**, 34992–34999.
24. Hud,N.V., Schultze,P. and Feigon,J. (1998) *J. Am. Chem. Soc.*, **120**, 6403–6404.
25. Hud,N.V., Schultze,P., Sklenár,V. and Feigon,J. (1999) *J. Mol. Biol.*, **285**, 233–243.
26. Phillips,K., Dauter,Z., Murchie,A.I.H., Lilley,D.M.J. and Luisi,B. (1997) *J. Mol. Biol.*, **273**, 171–182.
27. Laughlan,G., Murchie,A.I.H., Norman,D.G., Moore,M.H., Moody,P.C.E., Lilley,D.M.J. and Luisi,B. (1994) *Science*, **265**, 520–524.
28. Smith,F.W. and Feigon,J. (1993) *Biochemistry*, **32**, 8682–8692.
29. Sandström,J. (1982) *Dynamic NMR Spectroscopy*, Academic Press, New York, NY.
30. de Leeuw,F.A.A.M. and Altona,C.J. (1983) *J. Comp. Chem.*, **4**, 428–437.
31. Schultze,P. and Feigon,J. (1997) *Nature*, **387**, 668.
32. Hud,N.V., Smith,F.W., Anet,F.A.L. and Feigon,J. (1996) *Biochemistry*, **35**, 15383–15390.
33. Brünger,A.T. (1992) *X-PLOR (Version 3.1) Manual*. Yale University Press, New Haven, CT.
34. Detellier,C. and Laszlo,P. (1980) *J. Am. Chem. Soc.*, **102**, 1135–1141.
35. Sundquist,W.I. and Klug,A. (1989) *Nature*, **342**, 825–829.
36. Hud,N.V., Sklenár,V. and Feigon,J. (1999) *J. Mol. Biol.*, **286**, 651–659.
37. Strahan,G.D., Keniry,M.A. and Shafer,R.H. (1998) *Biophys. J.*, **75**, 968–981.
38. Smith,F.W., Lau,F.W. and Feigon,J. (1994) *Proc. Natl Acad. Sci. USA*, **91**, 10546–10550.
39. Keniry,M.A., Strahan,G.D., Owen,E.A. and Shafer,R.H. (1995) *Eur. J. Biochem.*, **233**, 631–643.
40. Bouaziz,S., Kettani,A. and Patel,D.J. (1998) *J. Mol. Biol.*, **282**, 637–652.
41. Piotto,M., Saudek,V. and Sklenár,V. (1992) *J. Biomol. NMR*, **2**, 661–665.